



Global carbon emission accounting: national-level assessment of wildfire CO₂ emission—a case study of China

Xuehong Gong^{1,2}, Zeyu Liu^{2,3}, Jie Tian^{2,3}, Qiyuan Wang^{2,3}, Guohui Li^{2,3}, Zhisheng An^{1,2}, Yongming Han^{2,3*}

5 ¹ State Key Laboratory of Earth Surface Processes and Resource Ecology, Faculty of Geographical Science, Beijing Normal University, Beijing 100875, China

² State Key Laboratory of Loess and Quaternary Geology, Institute of Earth Environment, Chinese Academy of Sciences, Xi'an 710061, China

10 ³ National Observation and Research Station of Regional Ecological Environment Change and Comprehensive Management in the Guanzhong Plain, Xi'an 710061, China

Correspondence to: Yongming Han (yongming@ieecas.cn)

Abstract. Wildfires release large amounts of greenhouse gases into the atmosphere, exacerbating climate change and causing severe impacts on air quality and human health. Including carbon dioxide (CO₂) emissions from wildfires in international assessments and national emission reduction responsibilities is crucial for global carbon reduction and environmental governance. In this study, based on a bottom-up approach and using satellite data, combined with emission factor and aboveground biomass data for different vegetation cover types (forest, shrub, grassland, cropland), the dynamic changes in CO₂ emissions from wildfires in China from 2001 to 2022 were analyzed. The results showed that between 2001 and 2022, the total CO₂ emissions from wildfires in China were 693.7 Tg (1 Tg = 10¹² g), with an annual average of 31.5 Tg. The CO₂ emissions from cropland and forest fires were relatively high, accounting for 46% and 32%, respectively. The yearly variation in CO₂ emissions from forest and shrub fires showed a significant downward trend, while emissions from grassland fires remained relatively stable. In contrast, the CO₂ emissions from cropland fires showed a clear upward trend. High CO₂ emissions from wildfires were mainly concentrated in the eastern regions of Heilongjiang and Inner Mongolia Provinces in China, accounting for 44% of the total annual emissions. Various factors such as daily cumulative sunshine hours (Spearman's correlation coefficient, forest: -0.41, shrub: 0.25; $p < 0.001$) and the normalized difference vegetation index (NDVI; Spearman's correlation coefficient, forest: -0.35, shrub: 0.37; $p < 0.001$), influenced CO₂ emissions from forest and shrub fires. Moreover, temperature (Spearman's correlation coefficient, -0.45, $p < 0.001$) primarily affected CO₂ emissions from grassland fires. The CO₂ emissions from cropland fires negatively correlated with the gross domestic product (GDP) (Spearman's correlation coefficient, -0.52, $p < 0.001$) and population density (Spearman's correlation coefficient, -0.51, $p < 0.001$). China's policy management has been crucial in reducing CO₂ emissions from wildfires. By accurately assessing CO₂ emissions from wildfires, governments worldwide can better set CO₂ reduction targets, take corresponding measures, and contribute to the global response to climate change.



1 Introduction

To limit the global average surface temperature rise to 1.5 °C higher than preindustrial levels, carbon dioxide (CO₂) emissions must reach net zero by mid-century through various pathways (Rogelj et al., 2018). Globally, wildfires reduce carbon storage in vegetation by approximately 10% from 2001 to 2012 (Lasslop et al., 2020). This significantly impacted the concentration of CO₂ in the atmosphere (Langenfels et al., 2002; Van Der Werf et al., 2004; Wotawa and Trainer, 2000). The global annual CO₂ emissions from wildfires are approximately 6.5 to 11 billion tons, accounting for approximately one-fifth of the global CO₂ emissions from fossil fuels (Van Der Werf et al., 2010). However, the role of wildfires as a critical factor in carbon sequestration/sources is often overlooked. To mitigate climate change and fully understand the carbon exchange mechanisms between terrestrial ecosystems and the atmosphere, it is essential to consider the impacts of wildfire CO₂ emissions on the Earth system (Chuvieco et al., 2019; Giglio et al., 2018; Kasischke et al., 1995; McGuire et al., 2001; Zhang et al., 2013).

The significant differences in global wildfire CO₂ emissions among countries highlight the complexity of wildfire CO₂ emissions. Extreme forest fires in several countries, such as Australia, Canada, and the United States, often release CO₂ that exceeds the cumulative CO₂ emissions of several years in the same region, significantly impacting the global climate and the environment. Boreal fires, which usually contribute 10% of global fire CO₂ emissions, accounted for 23% in 2021 (0.48 billion metric tons of carbon), marking the highest fraction since 2000 (Zhang et al., 2023). The unprecedented wildfires in Canada in 2023 released significant amounts of air pollutants and greenhouse gases into the atmosphere. Simulation results (Wang et al., 2023) have indicated that these wildfires emitted more than 1300 Tg CO₂ and 140 Tg CO₂ equivalent of other greenhouse gases, including CH₄ and N₂O. The greenhouse gas emissions associated with wildfires exceeded twice the planned cumulative anthropogenic emissions reductions in Canada over a decade. Shiraishi et al. (2021) used a bottom-up approach to estimate CO₂ emissions from catastrophic fires in Australia between 2019 and 2020. The results showed that from March 2019 to February 2020, Australia's annual CO₂ emissions were estimated to be 806 ± 69.7 Tg CO₂ year⁻¹, equivalent to 1.5 times its total greenhouse gas emissions (CO₂ equivalent) in 2017. Phillips et al. (2022) reported that by the middle of this century, wildfires in northern North America could lead to a cumulative net source of approximately 12 billion tons of CO₂, accounting for approximately 3% of the remaining global CO₂ emissions, which is closely related to the temperature targets of the Paris Agreement. In the context of climate change, wildfires are becoming more frequent, and CO₂ emissions from wildfires are often influenced by human intervention. Phillips et al. (2022) found that increasing investment in fire management to avoid CO₂ emissions is equivalent to or lower than other mitigation strategies. Therefore, changes in fire management may impact global atmospheric CO₂ concentrations, and proactive management strategies effectively reduce CO₂ emissions (Kelly et al., 2013; Phillips et al., 2022; Van Wees et al., 2021). However, CO₂ emissions from wildfires are not included in international assessments or national emission reduction responsibilities. Including wildfire CO₂ emissions in international assessments and national emission reduction responsibilities is crucial for global carbon reduction and environmental governance.



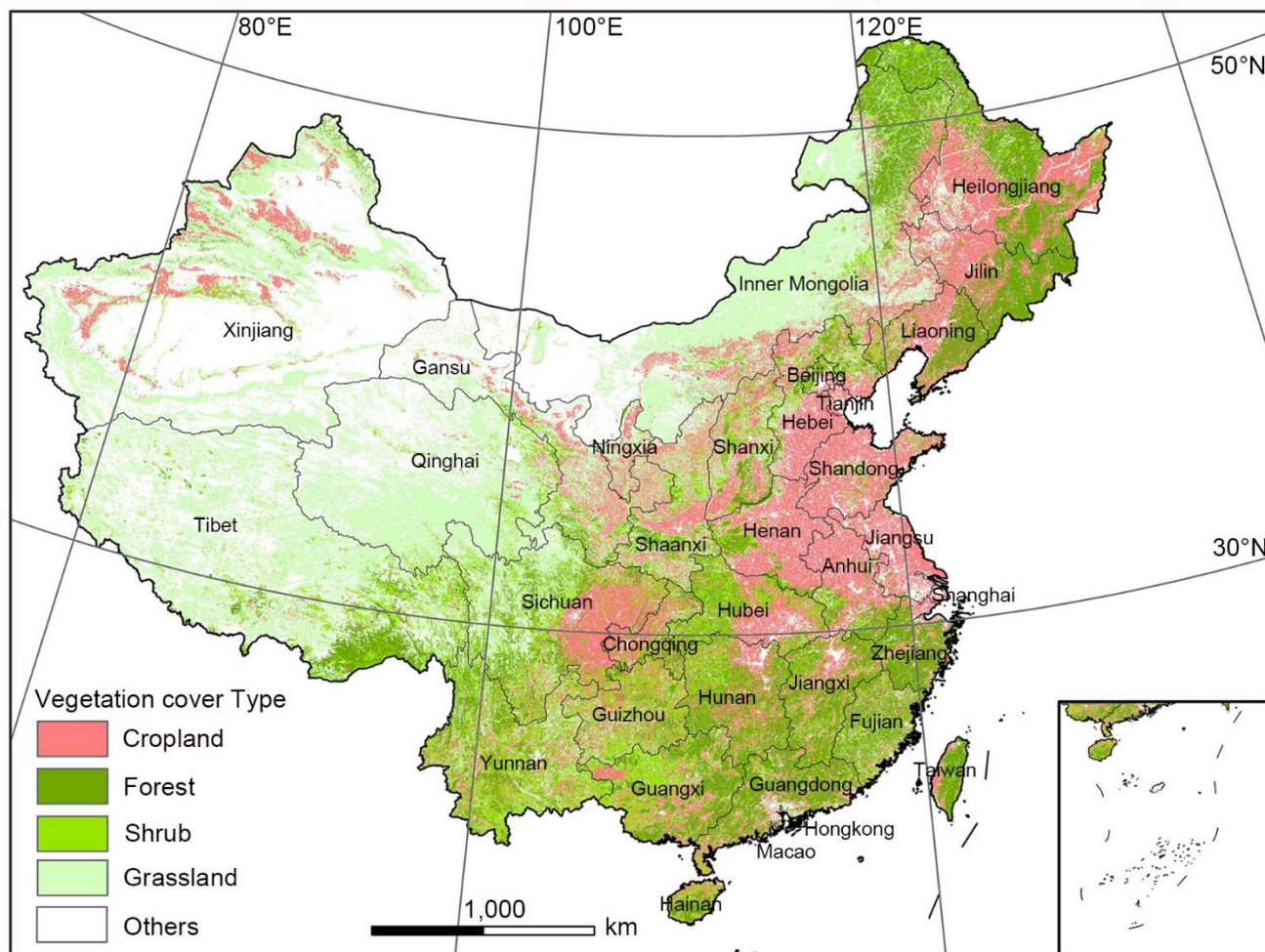
65 China has released a large amount of wildfire emission inventory, but previous research on wildfire emissions in China
has focused chiefly on small-scale and short-term periods (Cao et al., 2005; Huang et al., 2012; Qiu et al., 2016; Tian et al.,
2011; Wu et al., 2018). Wang et al. (2008) established an atmospheric pollutant emission inventory of cropland fires in
China in 2006 using the emission factor method and analyzed its spatiotemporal distribution characteristics. Wu et al. (2018)
estimated pollutant emission inventories from wildfires in central and eastern China from 2003 to 2015 using remote sensing
70 images but did not include the heavily polluted northeast region. In addition, most studies have focused mainly on
atmospheric pollutant emissions, with limited research on CO₂ emissions (Jin et al., 2022; Wang et al., 2008; Xie et al., 2024;
Yin et al., 2019). Xie et al. (2024) used the GEOS-Chem model to investigate the impact of cropland fires on severe haze
events in Heilongjiang Province. They reported high uncertainty in the existing Global Fire Emissions Database (GFED)
version 4.1 emission inventory. Van Der Werf et al. (2017) also noted substantial uncertainty in estimating wildfire
75 emissions in existing emission inventories. Therefore, more work must be done to explore the long-term dynamics of
wildfire emissions.

This study estimated the CO₂ emissions from wildfires, including forest, shrub, grassland, and cropland fires in China
from 2001 to 2022. Also, it explored the factors that may affect the spatiotemporal changes in CO₂ emissions from wildfires.
The study results can provide high spatial resolution and long-term wildfire CO₂ emission inventories, which can enhance
80 the accuracy of models assessing the impacts of wildfires on air quality, climate, and human health. Furthermore, this study
provides essential scientific support for air pollution control strategies and is a critical foundation for accurately evaluating
CO₂ emission reduction targets in various countries.

2 Data and methods

2.1 Study area

85 China is located in the eastern part of the Eurasian continent on the west coast of the Pacific Ocean. It spans
approximately 50 degrees (3-53 °N) from north to south and 60 degrees (73-135 °E) from east to west, with a land area of
approximately 9.60×10^6 km². There are differences in the distribution of cropland, grassland, shrubs, and forests in China.
Croplands are mainly located in the eastern plains and coastal areas, such as Northeast (Heilongjiang, Jilin, and Liaoning),
North (Hebei), and East (Shandong, Jiangsu) China, where the terrain is flat and suitable for agriculture. Grasslands are
90 mainly distributed in North (such as Inner Mongolia and Xinjiang) and Southwest (such as the western Sichuan Plateau) of
China, forming a vast grassland ecosystem. Shrubs are mainly distributed in mountainous and semiarid areas. Forests are
mainly distributed in Northeast (Heilongjiang, Jilin, and Liaoning) and Southwest (Yunnan, Guizhou) China, which have
abundant forest resources.



95 **Figure 1: Regional divisions and vegetation distribution in China.**

2.2 Data

The burned area data for wildfires with a spatial resolution of 500 m were sourced from MODIS-MCD64A1 burned area product (Giglio et al., 2018). The vegetation cover data were sourced from the China Land Use Land Cover Remote Sensing Monitoring Dataset (CNLUCC), with a spatial resolution of 30 m (Xu et al., 2018). A 1 km harvesting area dataset for three staple crops (e.g., corn, wheat, and rice) in China from 2000 to 2019 was obtained from Luo et al. (2020). Vegetation cover data were combined with fire area data to extract spatial data, including the time and geographic coordinates of fire occurrence, burned area, and vegetation cover types (corn, wheat, rice, grassland, shrub, and forest). The meteorological data were obtained from the Daily Meteorological Dataset of Essential Meteorological Elements of the China National Surface Weather Station (V3.0), and the spatial distribution of the meteorological data was calculated using the Kriging interpolation method in the ArcGIS 10.8 environment. The vegetation cover fraction was sourced from China's

100

105



regional 250 m fractional vegetation cover dataset (Gao et al., 2024a). The normalized difference vegetation index (NDVI) data were sourced from China's regional 250 m normalized difference vegetation index dataset (Gao et al., 2024b).

2.3 Methods

2.3.1 Emission factors

110 The emission factor refers to the gas released per unit mass of dry combustible material during combustion, typically in grams per kilogram (g kg^{-1}). This is a crucial parameter for calculating gas emissions during biomass burning, such as CO_2 , methane (CH_4), and carbon monoxide (CO). Emission factors are influenced by various factors, including the combustibility of tree species, differences in vegetation cover types, and the intensity of flame combustion (Andreae and Merlet, 2001; Lü et al., 2006). To ensure the accuracy of the wildfire emission inventory as much as possible, it is essential to choose
115 appropriate emission factors. This study comprehensively analyzed many studies in the literature to summarize the emission factors of CO_2 generated by wildfires under different vegetation cover types, as listed in Table S1. Finally, the average values from the literature were selected as the emission factors of the different vegetation cover types.

2.3.2 Aboveground biomass

Previous studies have mainly used the aboveground biomass data from Fang et al. (1996) for forests. Forest
120 aboveground biomass data in recent years need to be updated. In this study, the aboveground biomass data of shrubs and forests from 2001 to 2012 were obtained from Su et al. (2016). The data for 2013 to 2022 were obtained from Yan et al. (2023). Grassland aboveground biomass was calculated using the exponential model by Gao et al. (2012):

$$AGB_{grass} = 20.1921 \times e^{3.2154 \times (NDVI)} \quad (1)$$

where AGB_{grass} is the aboveground biomass of grassland (g m^{-2}) based on the average NDVI value of the growing season.

125 The aboveground biomass of cropland was obtained by multiplying the crop-specific yield per unit area by the straw-to-product ratio. The crop-specific yield per unit area (rice, corn, wheat) was derived from the China Statistical Yearbook, while the crop-specific yield per unit area of other crops was defined as the average of rice, corn, and wheat. The straw-to-product ratios for rice, wheat, corn, and other major crops were 1.323, 1.718, 1.269, and 1.5, respectively (Technical Guidelines for Compiling Emission Inventory of Air Pollutants from Biomass Combustion Sources, 2015).

130 2.3.3 Combustion efficiency

The combustion efficiency of biomass is an essential factor affecting the accuracy of wildfire CO_2 emission estimates. It is influenced by the intensity of fires, wildfire type, moisture content and load of combustibles, and meteorological conditions. Hély et al. (2003) established an empirical relationship between combustion efficiency and vegetation cover fraction (FVC). This relationship was applied in this study to the combustion efficiency calculation for forests, shrubs, and
135 grasslands.



$$CF = \begin{cases} 0.98 & \text{if } 40\% \leq FVC \text{ for grassland} \\ \exp(-0.13 \times FVC) & \text{if } 40\% < FVC \leq 60\% \text{ for grassland} \\ \exp(-1.3 \times FVC) & \text{if } T_c \leq 60\% \text{ for forest and shrub} \\ 0.25 & \text{if } FVC > 60\% \text{ for forest} \\ 0.3 & \text{if } FVC > 60\% \text{ for shrub} \\ 0.9 & \text{if } FVC > 60\% \text{ for grassland} \end{cases} \quad (2)$$

where CF is the combustion efficiency, and FVC is the vegetation cover fraction. The combustion efficiencies of corn, wheat, and rice were obtained from Zhou et al. (2017), with values of 0.92, 0.92, and 0.93, respectively. The combustion efficiency of other crops was taken as the average value for corn, wheat, and rice (i.e., 0.923).

140 2.3.4 CO₂ emission estimation

Using a bottom-up approach to estimate China's wildfire CO₂ emissions inventory, the wildfire CO₂ emissions are calculated using the following formula for forest, shrubs, and grasslands:

$$E_i = \sum_{x,i} BA_{x,i} \times AGB_{x,i} \times CF_i \times EF_i \quad (3)$$

145 where the subscripts x and i represent the location and vegetation cover type, respectively. E_i represents the CO₂ emission, $BA_{x,i}$ is the burned area (ha), $AGB_{x,i}$ is the aboveground biomass (t ha⁻¹), and EF_i is the emission factor. CF_i is the combustion efficiency.

For cropland fires, cropland was further divided into four categories: rice, wheat, corn, and others. The specific calculation formula is as follows:

$$E_j = \sum_{x,j} BA_{x,j} \times B_{x,j} \times N_j \times CF_j \times EF_j \quad (4)$$

150 where the subscripts x and j represent the location and type of crop, respectively. E_j represents the CO₂ emissions, $BA_{x,j}$ is the burned area, $B_{x,j}$ is the per hectare yield of crop type j at location x, N_j is the straw-to-product ratio, EF_j is the emission factor, and CF_j is the combustion efficiency.

3 Results and discussion

3.1 Interannual Variation in CO₂ Emissions

155 The total CO₂ emissions from wildfires in China from 2001 to 2022 were 693.7 Tg, with an average annual value of 31.5 Tg, accounting for 0.46% of the total global emission of All fire types (GFED4, all fire types mean of 7140 Tg from 2001 to 2022, Van Der Werf et al., 2017), and 0.52% of China's fossil fuel emission (approximately 6400 Tg, Shan et al., 2017). CO₂ emissions from wildfires in China were relatively low, decreasing slowly by 0.43 Tg per year (Fig. 2a). CO₂ emissions from cropland and forest fires were relatively high, accounting for 46% and 32%, respectively; shrub fires emissions account for 20%, while grassland fire emissions were the lowest, accounting for only 2% (Fig. 2b).

160

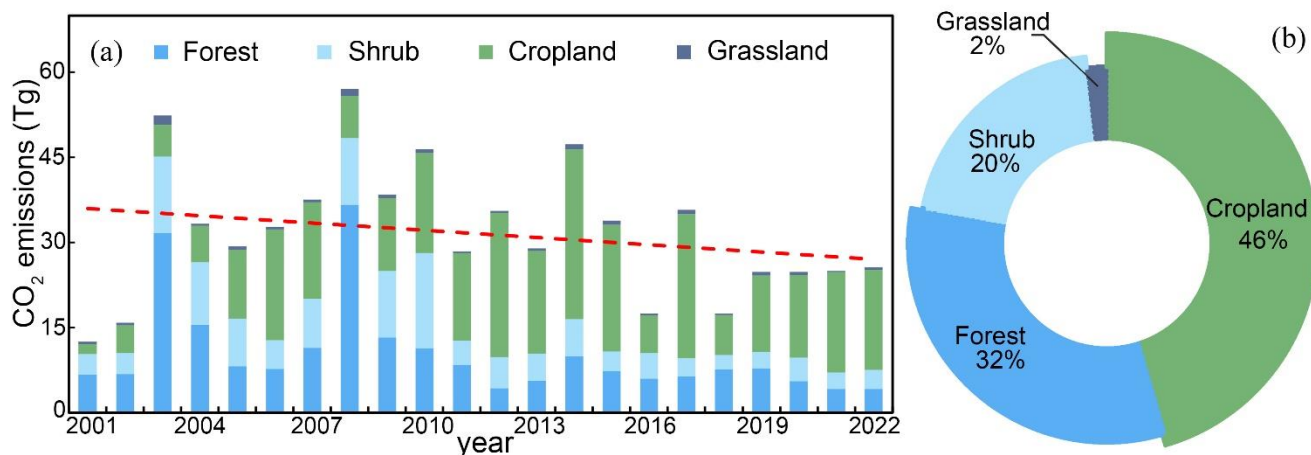
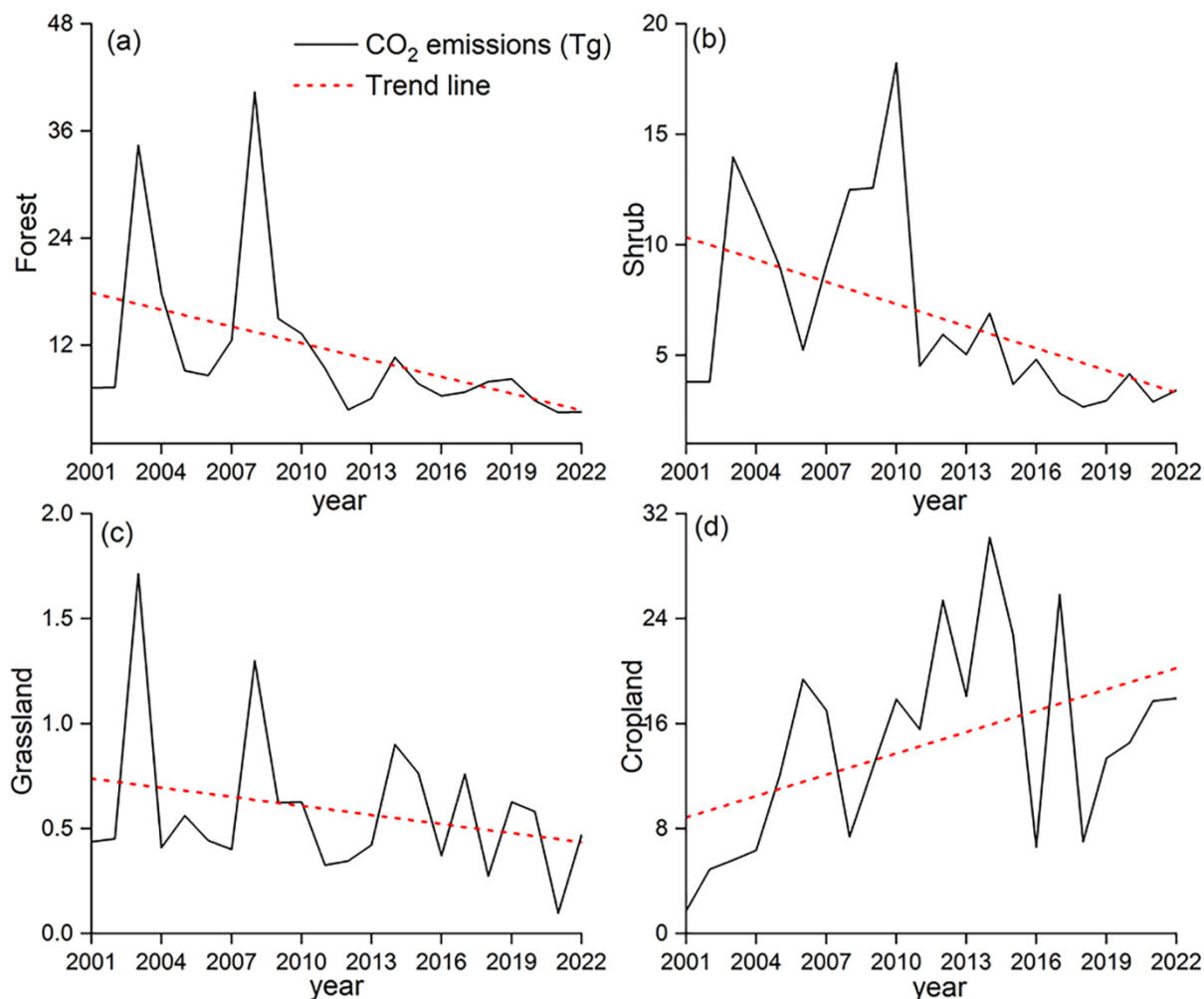


Figure 2: (a) Annual CO₂ emissions within specific vegetation cover types from 2001 to 2022 in China; (b) Contribution of different vegetation cover types to the total CO₂ emissions from 2001 to 2022 in China.

165 The annual CO₂ emissions from different types of fires showed varying temporal trends. The downward trend for forest and shrub emissions was significant, with a decrease of 0.63 and 0.33 Tg per year, respectively (Fig. 3a and 3b). Such a decline may reflect effective forestry management strategies for forest and shrub fires. In contrast, cropland emissions showed a clear upward trend, with an annual increase of 0.63 Tg (Fig. 3c). This may be related to an increase in agricultural activities, changes in land use, or an increase in cultivation intensity. The emission trend for grassland was relatively stable (Fig. 3d), which might be influenced by a combination of ecological and anthropogenic factors.



170

Figure 3: Time series of CO₂ emissions for different vegetation cover types from 2001 to 2022 in China: (a) Forest, (b) Shrub, (c) Grassland, (d) Cropland.

3.2 Monthly Variation in CO₂ Emissions

The CO₂ emissions from different vegetation cover types showed significant seasonal fluctuations, with certain months showing higher emissions than others. Wildfires had lower CO₂ emissions in July and August, which may correspond to the respective wet seasons. Wet conditions usually reduce the occurrence rate of fires (Fig. 4). Forest, shrub, and grassland fires had higher emissions in February, March, and April, possibly related to the dry weather and accumulation of combustible materials in spring, increasing the risk of fires. Cropland fires showed significant emission peaks in April, May, and June. This pattern may be related to specific agricultural activity (such as plowing, sowing, and harvesting) cycles, as cropland fires often occur after harvest when crop residues are burned to prepare for the next planting season. The spatial distribution of forest, shrub, and grassland fire emissions were relatively similar among the different months (Figs. S1-S3). In contrast,

175

180



185

the spatial distribution of emissions from cropland fires varied significantly across different months and was likely influenced by policy management (Fig. 5). The high emissions of cropland fires in March and April mainly originated from Heilongjiang and Jilin Provinces. The high emissions of cropland fires in May and June mainly came from the Anhui, Henan, and Jiangsu Provinces.

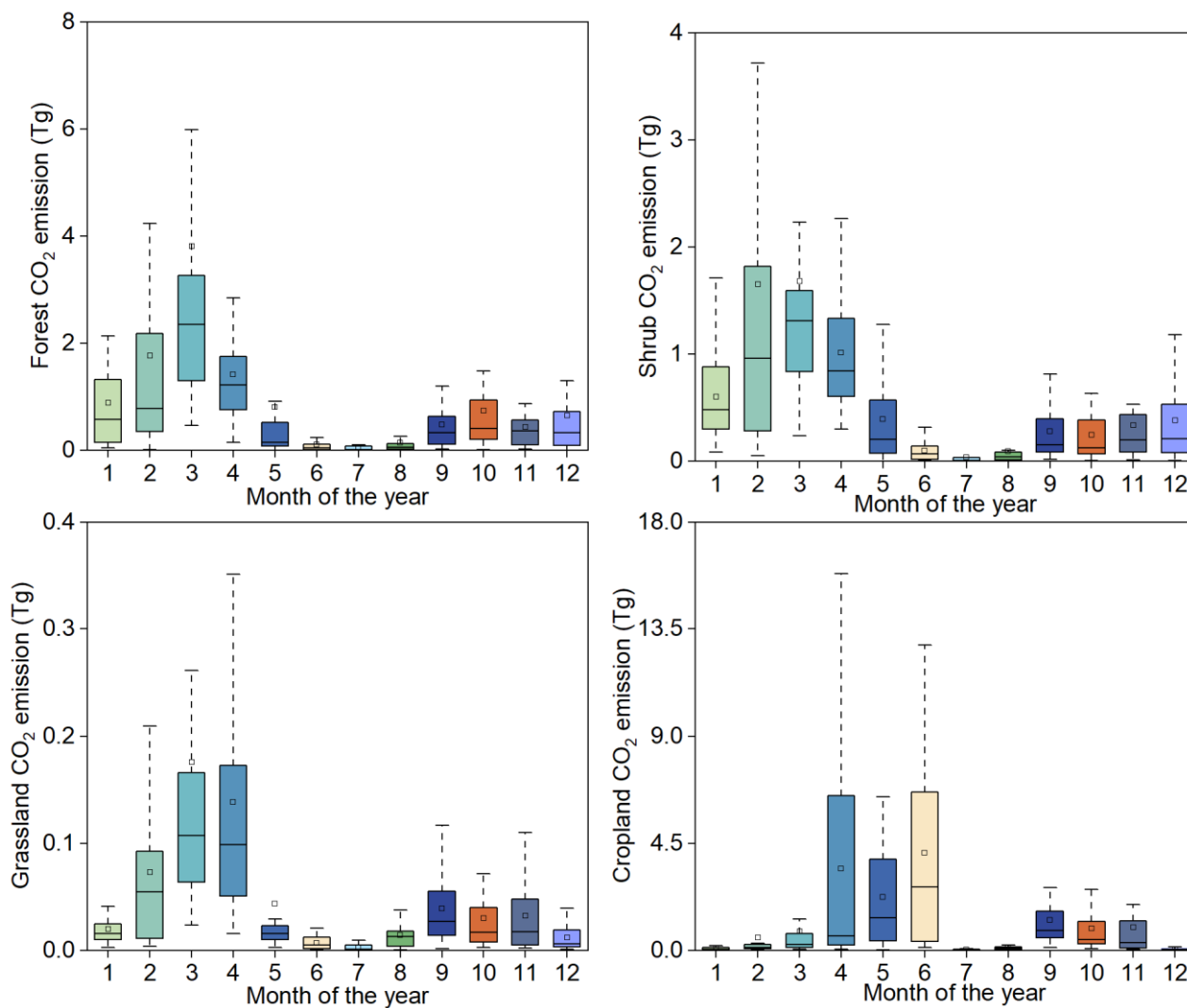
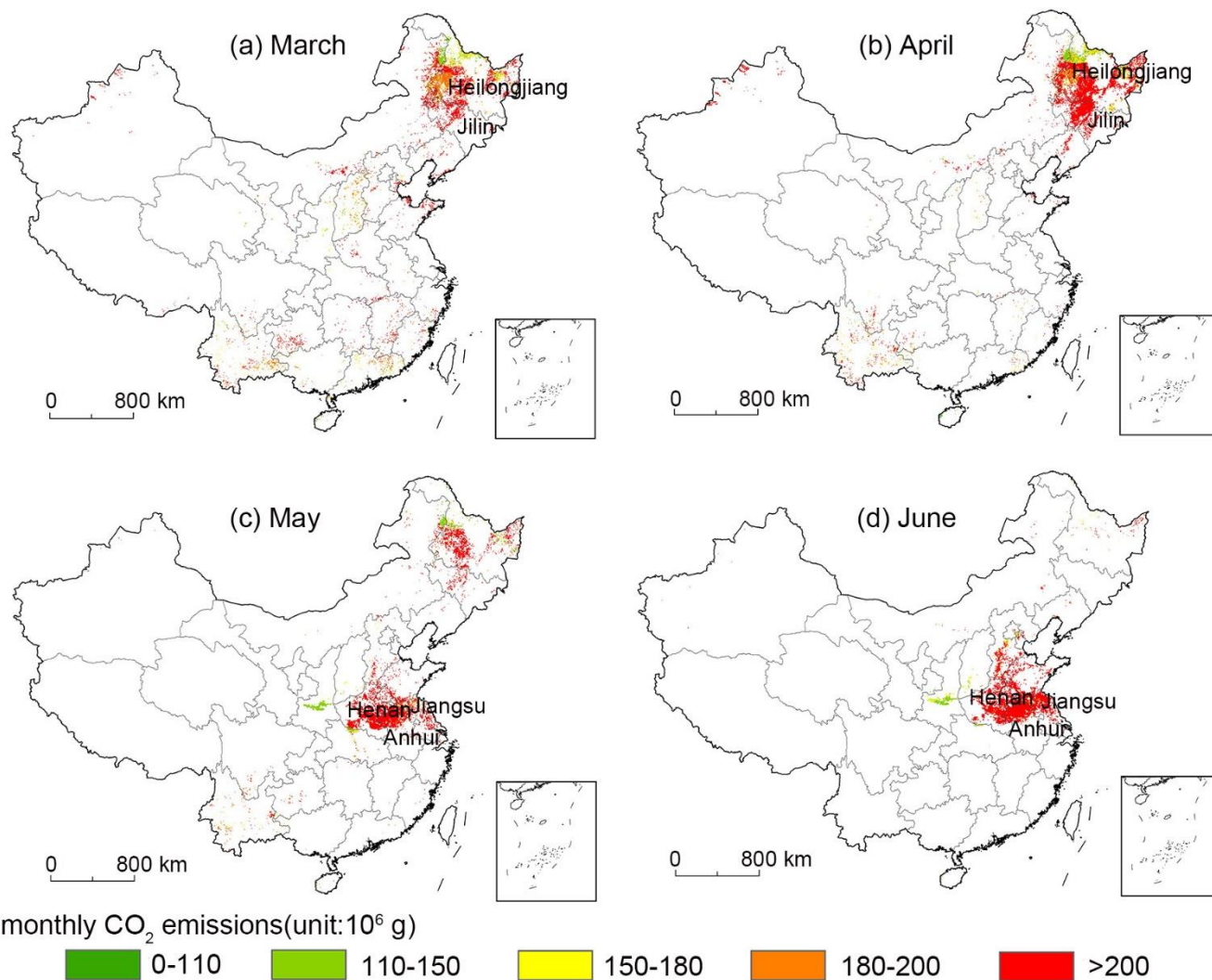


Figure 4: Box plots of CO₂ emissions for specific vegetation cover types per month from 2001 to 2022 in China, showing the median (black line), mean (box), and the range within 1.5 times the interquartile range (IQR): (a) Forest, (b) Shrub, (c) Grassland, (d) Cropland.



190

Figure 5: Spatial distribution of monthly CO₂ emissions within cropland fires from 2001 to 2022 in China: (a) March, (b) April, (c) May, and (d) June.

3.3 Spatiotemporal Variations in CO₂ Emissions

Due to differences in geographical location, climate conditions, and population density, the spatiotemporal distribution of CO₂ emissions in each region exhibits heterogeneity (Fig. 6). Overall, the emissions in the northwestern region of China were relatively low. The significant areas with higher emissions were mainly concentrated in China's eastern and central regions (Fig. 6a). The areas with high CO₂ emissions from forest fires were mainly in the northeast and southwest regions (Fig. 6b). The distribution of high CO₂ emissions from shrub fires was relatively scattered. However, there were some concentrated high-emission areas in the western and northeastern regions (Fig. 6c). The emissions from grassland fires were

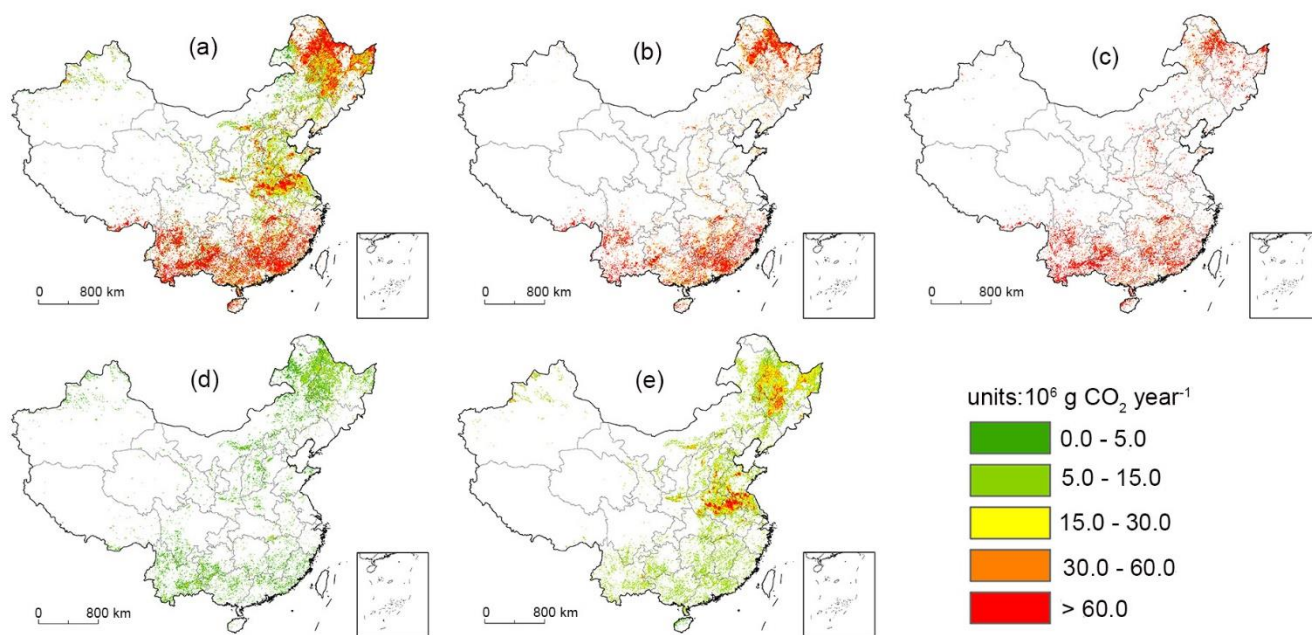


200 generally low and were mainly concentrated in Northeastern China (Fig. 6d). The high-value areas of CO₂ emissions from cropland fires were mainly concentrated in eastern China (Fig. 6e).

The results of the global spatial autocorrelation analysis of CO₂ emissions from wildfires are shown in Table 1. Under different wildfires, the p values were all less than 0.01, with a confidence level of 99%; the Moran's I values were all positive, with a Z score greater than 2.58, indicating a significant positive spatial autocorrelation of CO₂ emissions from wildfires, exhibiting an aggregation pattern in spatial distribution.

Table 1. Global spatial autocorrelation statistics of CO₂ emissions

Vegetation cover type	Moran's I	Z	P	Clustering pattern
Forest	0.052	5.072	0.000	Cluster
Shrub	0.118	8.961	0.000	Cluster
Grassland	0.064	6.632	0.000	Cluster
Cropland	0.281	20.414	0.000	Cluster
All	0.110	8.894	0.000	Cluster

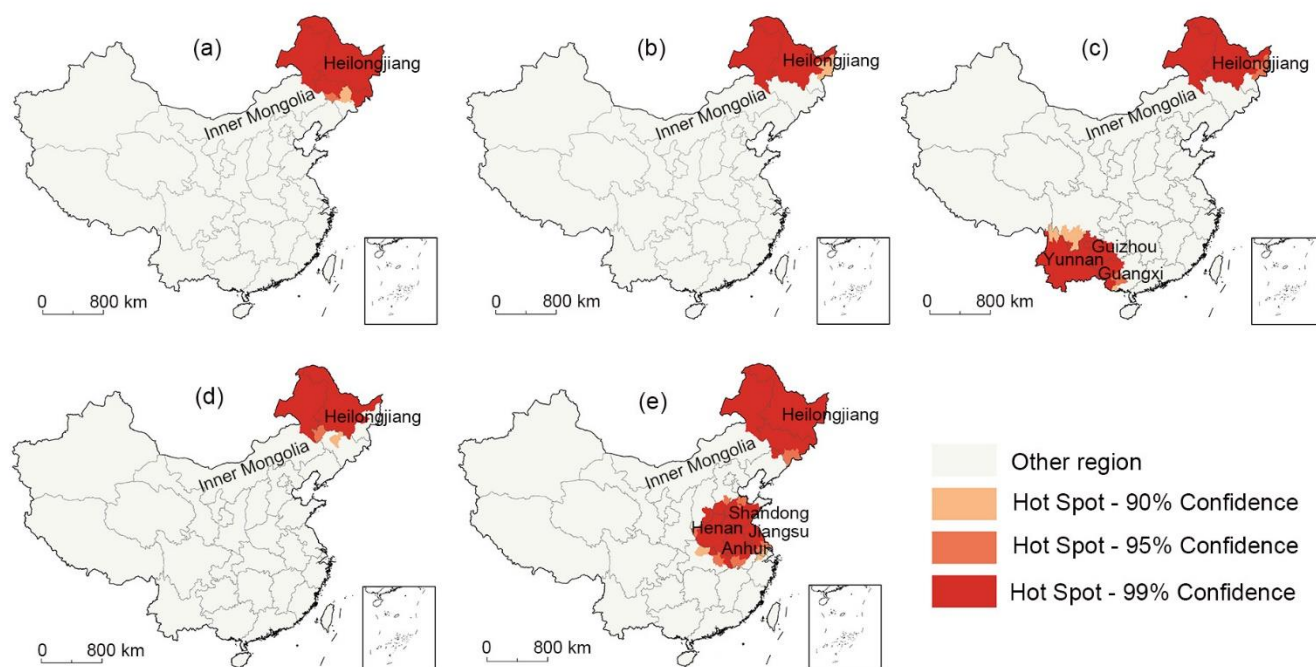


210 **Figure 6: Average annual spatial distribution of CO₂ emissions in China from 2001 to 2022: (a) all fire types, (b) Forest, (c) Shrub, (d) Grassland, and (e) Cropland.**

The hotspot analysis of wildfire CO₂ emissions investigated the specific spatial clustering of CO₂ emissions, as shown in Figure 7. In general, the high values of CO₂ emissions were mainly concentrated in the eastern regions of Heilongjiang and Inner Mongolia Provinces in China from 2001 to 2022, with annual emissions accounting for 44% of the total annual



emissions (Fig. 7a). There was only one high-value aggregation area for forest fires and grassland fires, which is similar to
 215 the spatial distribution of total emissions (Fig. 7b and Fig. 7d). The average annual emissions of high-value aggregation
 areas accounted for 53% and 64% of the total annual emissions, respectively. There were two high-value clusters of shrub
 fires, one in the eastern regions of Heilongjiang and Inner Mongolia Provinces and the other in the southwestern forest areas,
 with annual emissions accounting for 25.82% and 40% of the total emissions, respectively (Fig. 7c). There were also two
 high-risk areas for cropland fires, one in the eastern regions of Heilongjiang and Inner Mongolia Provinces and the other in
 220 the eastern and central regions of China, mainly including Shandong, Henan, Anhui, and Jiangsu (Fig. 7e). The average
 annual emissions accounted for 43% and 48% of the total emissions, respectively. It is worth noting that northeastern China
 is marked as a high-confidence hotspot area among all fire types, which may indicate the long-term existence of high CO₂
 emissions in the region.



225 **Figure 7: Spatial distribution of CO₂ emission hotspots from 2001 to 2022 in China: (a) all fire types, (b) Forest, (c) Shrub, (d) Grassland, and (e) Cropland.**

For emissions from different vegetation cover types, some years and regions exhibit unexpectedly high emissions, potentially caused by special events such as abnormal climate conditions, human activities, and fire management. Figure 8 shows the time series of high-emission regions under the different vegetation cover types from 2001 to 2022. Extreme forest
 230 fires occurred in Heilongjiang and Inner Mongolia Provinces in 2003, and the total emissions of these two provinces accounted for 73% of the total emissions in 2003 (Fig. 8a). The high emissions in 2008 were due to forest fires in Inner Mongolia, which accounted for 47% of the total emissions in 2008. Shrub fire emissions peaked in 2003 and 2010 (Fig. 8b).



The emissions in 2003 occurred mainly in Yunnan, Inner Mongolia, and Heilongjiang, with the total emissions from these three provinces accounting for 63% of the total emissions. The emissions in 2010 occurred mainly in Yunnan and Guizhou, accounting for 78% of the total emissions in 2010. Grassland fire emissions also peaked in 2003 and 2008, with the 2003 main emission areas being Inner Mongolia and Heilongjiang, accounting for 85% of the total emissions for that year. Inner Mongolia was the central emission region in 2008, accounting for 62% of the total emissions for that year (Fig. 8c). Human activities and fire management may affect cropland fire emissions more significantly, resulting in more significant variability in CO₂ emissions across provinces (Fig. 8d). Heilongjiang Province had relatively low emissions from 2001 to 2013, with emissions increasing and trending upward from 2014, where the annual average emissions from 2014 to 2022 were five times greater than the annual average emissions from 2001 to 2013. The primary emission years for the Anhui and Henan Provinces were between 2006 and 2014, with emissions decreasing after 2015. The emission trend in Jilin Province was similar to that in Heilongjiang Province, with higher emissions in recent years. In other regions, CO₂ emissions from cropland fires were relatively high before 2012. After the implementation of China's strict ban on open-air biomass burning in 2012, emissions decreased, showing an overall downward trend.

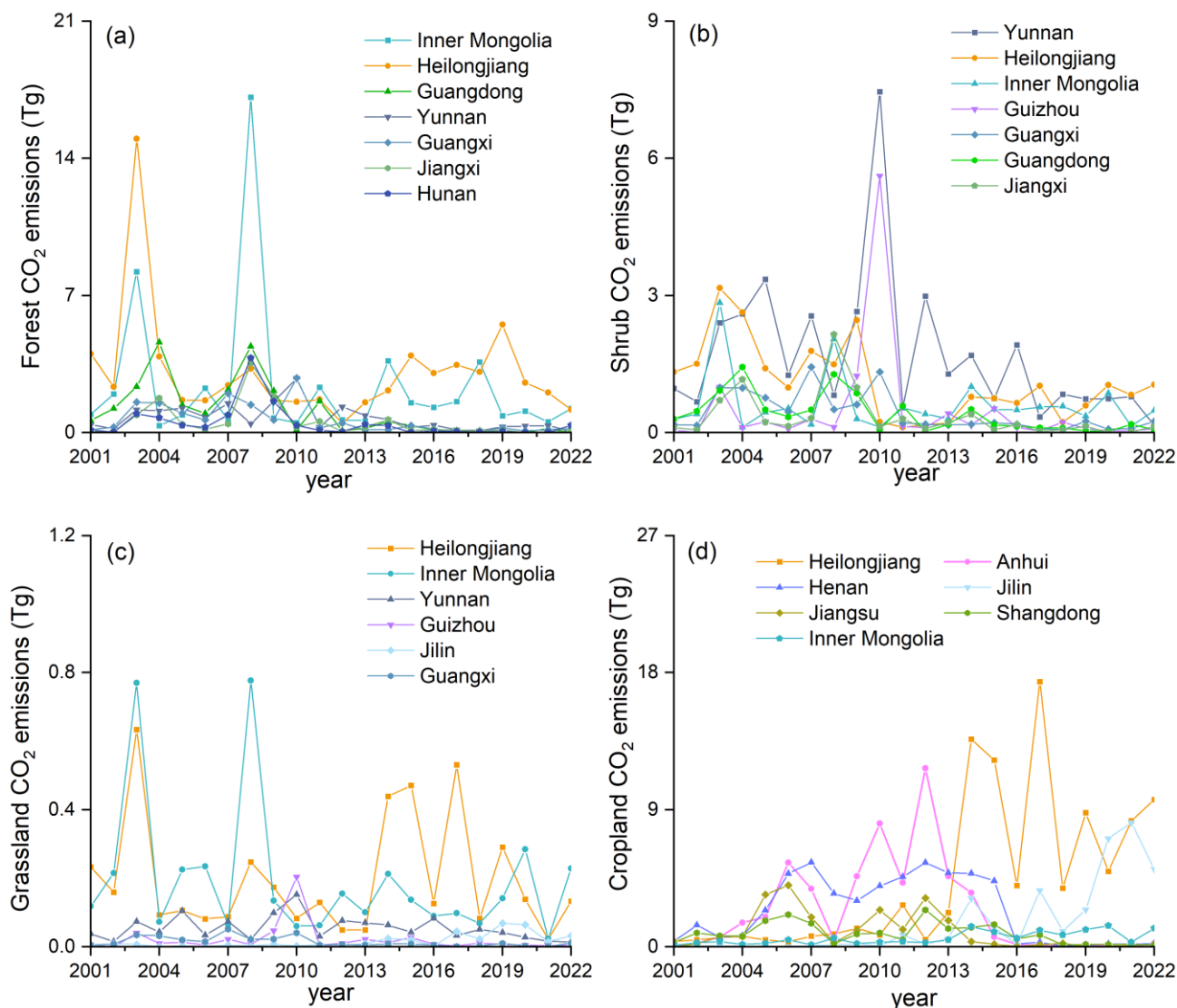
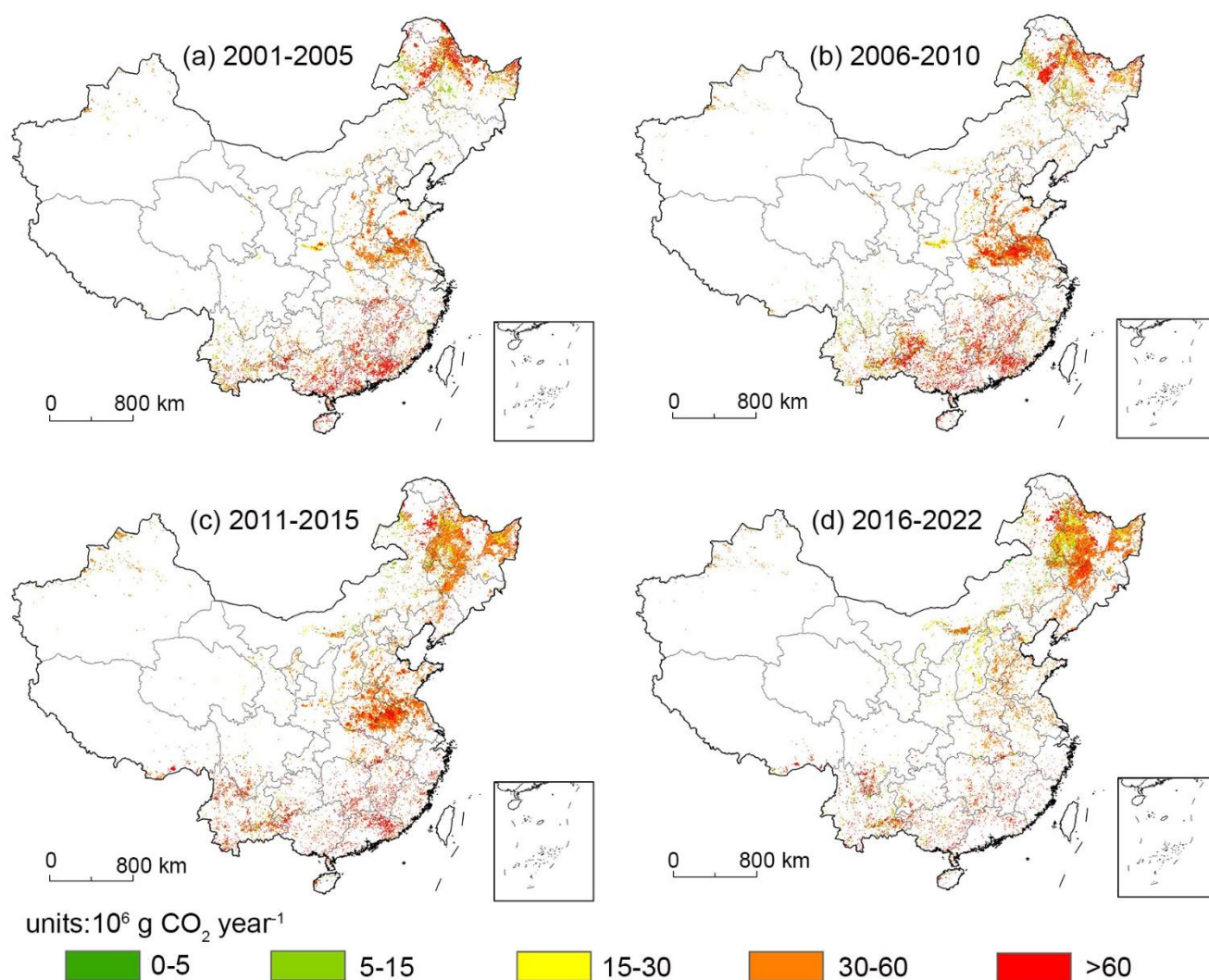


Figure 8: Time series of CO₂ emissions in major regions under different vegetation cover types from 2001 to 2022 in China: (a) Forest, (b) Shrub, (c) Grassland, and (d) Cropland.

The spatial distribution of CO₂ emissions changes over different periods from 2001 to 2022 (Fig. 9). The average annual CO₂ emission from 2001 to 2005 was 28.7 Tg, with CO₂ emission mainly concentrated in the eastern region of China (Fig. 9a). The average annual emissions from Heilongjiang and Inner Mongolia accounted for 42% of the total annual emissions. Compared with 2001-2005, the average annual CO₂ emissions increased from 2006 to 2010 (39.8 Tg), and the high-emission areas increased (Fig. 9b). High emissions still existed in Heilongjiang and Inner Mongolia in the east. However, other provinces, such as Anhui and Henan, began to show higher emissions, mainly due to an increase in cropland fires in these provinces (Figs. S4-S7). The average annual CO₂ emissions decreased from 2011 to 2015 (34.9 Tg). Forest fire



emissions in Heilongjiang and Inner Mongolia decreased, while cropland fire emissions increased (Figs. S4-S7). High CO₂ emissions from cropland fires still occurred in provinces such as Anhui and Henan (Fig. 9c). The average annual CO₂ emissions from 2016 to 2022 were the lowest of the four time periods (24.4 Tg), with an overall decrease in CO₂ emissions from forest, shrub, and grassland fires (Fig. 9d). CO₂ emissions from cropland fires in various provinces, such as Anhui and Henan, decreased, while high emissions from cropland fires in the eastern regions of Heilongjiang, Inner Mongolia, and Jilin still existed. The average annual emissions from Heilongjiang, Jilin, and Inner Mongolia accounted for 80% of the total annual emissions.



265 **Figure 9: Spatial distribution of annual CO₂ emissions for all types of fires from (a) 2001 to 2005, (b) 2005 to 2010, (c) 2011 to 2015, and (d) 2016 to 2022.**

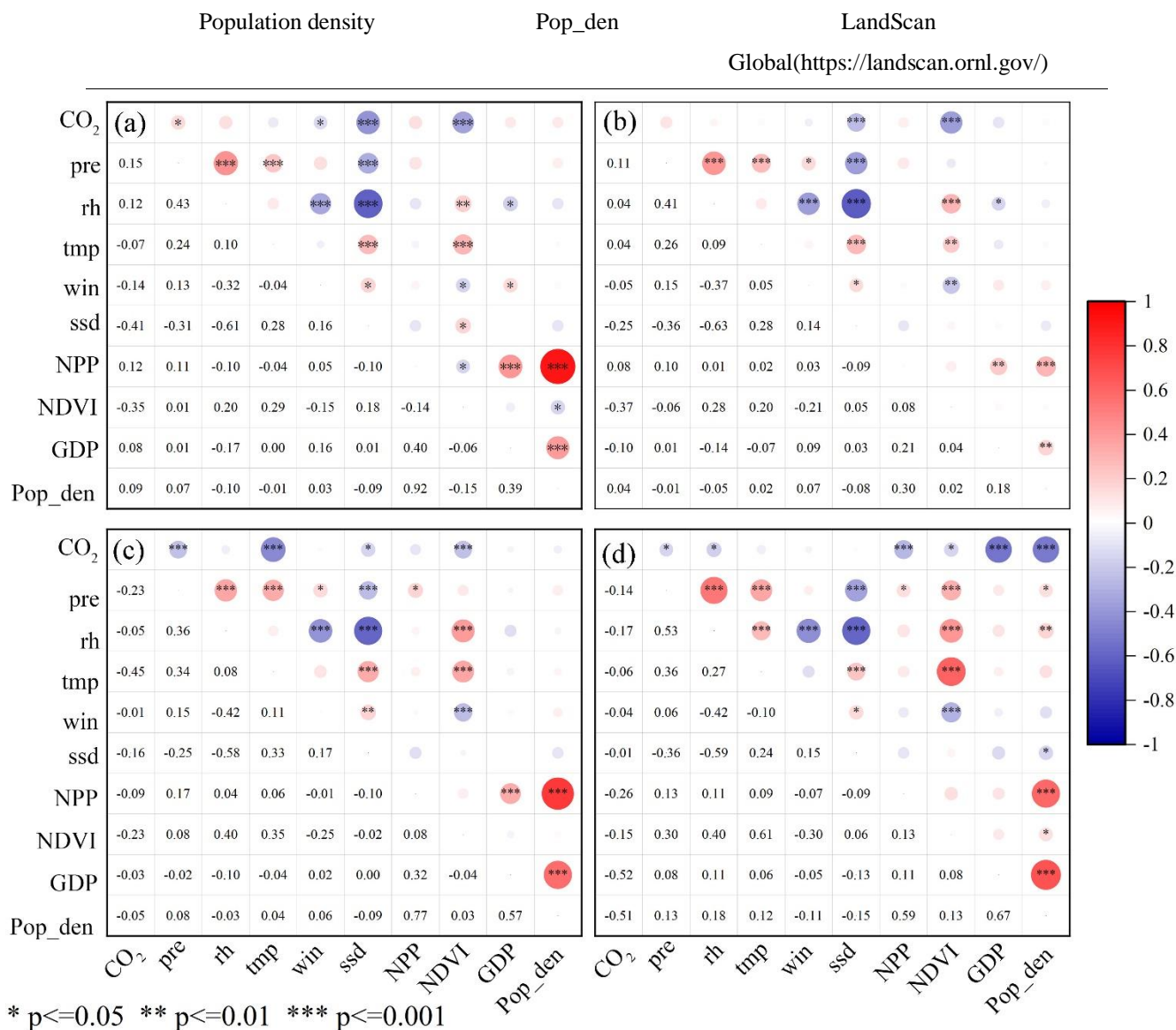


3.4 The impact of factors on wildfires in China

The factors influencing CO₂ emissions from wildfires are numerous and complex. The Spearman correlation coefficient method was utilized to analyze the connection between CO₂ emissions from wildfires in China and various climate factors, such as temperature, precipitation, relative humidity, wind speed, sunshine, and vegetation factors, including vegetation primary productivity and the NDVI. Additionally, the gross domestic product (GDP) and population density were taken into account (Fig. 10). The main factors influencing CO₂ emissions from forest and shrub fires were daily cumulative sunshine hours (forest:-0.41, shrub:0.25; $p < 0.001$) and NDVI (forest:-0.35, shrub:0.37; $p < 0.001$), while the main factor affecting CO₂ emissions from grassland fires was temperature (-0.45, $p < 0.001$) (Fig. 10a-c). Cropland fires, influenced by human activities, showed a specific negative correlation with GDP (-0.52, $p < 0.001$) and population density (-0.51, $p < 0.001$). At the same time, other factors had relatively small impacts (Fig. 10d). An increase in GDP and population density was often accompanied by better agricultural technology and management practices, including more effective management alternatives to straw burning. Furthermore, changes in fire management may impact CO₂ emissions from wildfires (Gao et al., 2023; Jin et al., 2022; Kelly et al., 2013; Phillips et al., 2022; Van Wees et al., 2021; Xie et al., 2024). Phillips et al. (2022) found that the cost of avoiding CO₂ emissions by increasing investment in fire management is comparable to or lower than that of other mitigation strategies. China's policies have also significantly reduced CO₂ emissions from opening biomass burning fires. Since the forest fire broke out in the Greater Khingan Mountains region of China on May 6, 1987, China has implemented a forest fire prevention and control policy of "prevention first, active elimination." Subsequently, local governments have introduced specific policies on forest, shrub, and grassland fire prevention, successfully reducing the occurrence of forest and shrub fires in China. The research in this paper also showed that the trend in CO₂ emissions from forest and shrub fires had decreased significantly since 2001 (Fig. 3a and 3b). Moreover, Jin et al. (2022) reported that from 2001 to 2019, compared with those of natural wildfires (without strict wildfire management), the average CO₂ emissions generated by wildfires (forest, shrub, and grassland fires) under management policies decreased by more than 80%.

Table 2 Driving factors and sources

Driving factors	Abbreviation	Source
Punctual temperature	tmp	
Relative humidity	rh	Daily meteorological dataset of essential meteorological elements of China National Surface Weather Station (V3.0)
Accumulated precipitation	pre	
Wind speed (2 m)	win	
Daily cumulative sunshine hours	ssd	
Vegetation primary productivity	NPP	MODIS MOD17A3
Normalized Difference Vegetation Index	NDVI	National Qinghai Tibet Plateau Science Data Center
Gross domestic product	GDP	Chen et al. (2022)



290 **Figure 10: Heatmap of Spearman's correlation coefficients between pairs of variables: (a) forest; (b) shrub; (c) grassland; (d) cropland** See Table 2 for variable descriptions.

3.5 Implications

The burning of agricultural straw in China is a long-standing phenomenon, where burning straw is a traditional method for farmers to deal with waste straw after harvest. In recent years, the frequent occurrence of haze weather has seriously impacted people's production and life. Consequently, the government has introduced multiple policies to strengthen air quality and straw management. Since 2012, following the implementation of policies for air pollution prevention and control,

295



CO₂ emissions from cropland fires have decreased (Fig. 7d). However, some provinces, such as Heilongjiang and Jilin, have had higher emissions since 2012 and are on an upward trend (Fig. 7d). In the northeastern region, a large amount of straw is used as the primary non-commercial energy source, leading to serious straw burning issues. Cropland fires in Northeast China mainly occur during the harvest and crop sowing seasons, with peak burning periods in October-November and March-April. Although China has recently prohibited open-air straw burning, this phenomenon persists, indicating that crop straw remains the primary fuel and waste of rural residents. More research is needed to develop new solutions for the sustainable utilization of crop straw in the northeast region, which may help achieve the dual goals of improving air quality and mitigating climate change.

This study holds great significance for atmospheric pollution control management. First, the high spatial resolution and long time series of wildfire CO₂ emissions provide accurate input data for simulating the effects of wildfires on air quality, climate, and human health. This helps to gain a deeper understanding of the impact mechanism of wildfires on the atmospheric environment, providing a reliable foundation for related research. Second, this research has a direct impact on global climate governance. The natural process of carbon emissions from wildfires is essential to the global carbon cycle, with prominent human intervention and control properties. Reducing wildfire carbon emissions is also a potential means of reducing global carbon emissions. However, the current international assessment and national emission reduction responsibilities do not include wildfire carbon emissions or consider measures such as reducing wildfire frequency and intensity through wildfire management. By accurately assessing CO₂ emissions from wildfires, governments worldwide can better set CO₂ reduction targets, take corresponding response measures, and contribute to the global response to climate change.

4 Conclusion

Based on a bottom-up approach and using MODIS fire products combined with emission factors of different wildfires (forest, shrub, grassland, cropland), the dynamic changes in CO₂ emissions in China from 2001 to 2022 were analyzed. Overall, during this period, the total CO₂ emissions from wildfires in China amounted to 693.7 Tg, with average annual emissions of 31.5 Tg. The CO₂ emissions from cropland and forest fires were relatively high, accounting for 46% and 32%, respectively; Shrub fire emissions accounted for 20%, while grassland fire emissions were the lowest, accounting for only 2%. The study revealed that emissions from forest and shrub fires exhibited a significant downward trend. In contrast, emissions from grassland fires remained relatively stable, and cropland fire emissions showed a noticeable upward trend. The emissions also showed different characteristics in different months, with generally lower emissions from all types of fires in July and August. Forest, shrub, and grassland fires had higher emissions in February, March, and April, and cropland fire emissions peaked in April, May, and June, possibly correlated with specific agricultural activities. Spatially, high CO₂ emissions were primarily concentrated in the eastern regions of Heilongjiang and Inner Mongolia, accounting for 44% of the annual average total emissions. Northeast China was also identified as a high-confidence hotspot, indicating long-term high



CO₂ emissions. Human activities significantly influence CO₂ emissions from cropland fires. Emissions negatively correlated
330 with GDP (-0.52) and population density (-0.51). Various factors, such as accumulated sunshine hours (-0.41, $p < 0.001$) and
the NDVI (-0.35, $p < 0.001$), mainly influenced emissions from forest and shrub fires, while temperature (-0.45, $p < 0.001$)
primarily affected emissions from grassland fires. China's policy management has been crucial in reducing CO₂ emissions
from wildfires. By accurately assessing CO₂ emissions from wildfires, governments worldwide can better set CO₂ reduction
targets, take corresponding response measures, and contribute to the global response to climate change.

335 **Acknowledgments**

This work was supported by the National Natural Science Foundation of China (42221003 and 41991250), the Strategic
Priority Research Program of Chinese Academy of Sciences (XDB40000000).

Data availability

All the data supporting the findings of this paper can be accessed via the provided links or by requesting them using the
340 contact information provided within those links. The China Land Use Land Cover Remote Sensing Monitoring Dataset
(CNLUCC) is sourced from the Resource and Environment Science Data Registration and Publishing System
(<https://www.resdc.cn/>, last access: 4 June 2024). China's regional 250 m fractional vegetation cover dataset, China's
regional 250 m normalized difference vegetation index dataset, and The Daily Meteorological Dataset of Essential
345 Meteorological Elements of the China National Surface Weather Station (V3.0) are sourced from the National Tibetan
Plateau/Third Pole Environment Data Center (<https://data.tpsc.ac.cn/>, last access: 4 June 2024). MODIS-MCD64A1 burned
area data are publicly available at <https://lpdaac.usgs.gov/products/mcd64a1v061> (last access: 4 June 2024). A 1 km
harvesting area dataset is available at <http://dx.doi.org/10.17632/jbs44b2hrk.2> (last access: 4 June 2024).

Author contributions

The article was written with contributions from all the authors. Xuehong Gong and Yongming Han designed this study;
350 Xuehong Gong, Zeyu Liu, Jie Tian, and Qiyuan Wang collected and organized the data; Xuehong Gong analyzed the data
and wrote the original article with contributions from Zeyu Liu, Yongming Han, Guohui Li, and Zhisheng An. Zeyu Liu, Jie
Tian, and Qiyuan Wang assisted with the submission of the article. All the authors have given approval to the final version
of the article.

Competing interests

355 The contact author has declared that none of the authors has any competing interests.



References

- Andreae, M. O. and Merlet, P.: Emission of trace gases and aerosols from biomass burning, *Global Biogeochem. Cy.*, 15, 955–966, <https://doi.org/10.1029/2000GB001382>, 2001.
- Cao, G., Wang, F., and Wang, Y.: Emission inventory of TSP, PM₁₀ and PM_{2.5} emissions from biomass burning in China, *The Chinese Journal of Process Engineering*, 4, 700–704, 2004 (in Chinese).
- 360 Chuvieco, E., Mouillot, F., Van Der Werf, G. R., San Miguel, J., Tanase, M., Koutsias, N., García, M., Yebra, M., Padilla, M., Gitas, I., Heil, A., Hawbaker, T. J., and Giglio, L.: Historical background and current developments for mapping burned area from satellite Earth observation, *Remote Sens. Environ.*, 225, 45–64, <https://doi.org/10.1016/j.rse.2019.02.013>, 2019.
- Fang, J., Liu, G., and Xu, S.: Biomass and net production of forest vegetation in China, *Acta. Eco. Sin.*, 16, 497–508, 1996
- 365 (in Chinese).
- Gao, J., Chen, Y., Lü, S., Feng, C., Chang, X., Ye, S., and Liu, J.: A ground spectral model for estimating biomass at the peak of the growing season in Hulunbeier grassland, Inner Mongolia, China, *Int. J. Remote Sens.*, 33, 4029–4043, <https://doi.org/10.1080/01431161.2011.639401>, 2012.
- Gao, J., Yang, Y., Wang, H., Wang, P., Li, B., Li, J., Wei, J., Gao, M., and Liao, H.: Climate responses in China to domestic
- 370 and foreign aerosol changes due to clean air actions during 2013–2019, *npj Clim. Atmos. Sci.*, 6, 160, <https://doi.org/10.1038/s41612-023-00488-y>, 2023.
- Gao, J., Zhang, H., Zhang, W., Chen, X., Shen, W., Xiao, T., Zhang, Y., and Shi, Y.: China regional 250m fractional vegetation cover data set (2000–2023), <https://doi.org/10.11888/Terre.tpd.300330>, 2024a.
- Gao, J., Zhang, H., Zhang, W., Chen, X., Shen, W., Xiao, T., Zhang, Y., and Shi, Y.: China regional 250m normalized
- 375 difference vegetation index data set (2000–2023), <https://doi.org/10.11888/Terre.tpd.300328>, 2024b.
- Giglio, L., Boschetti, L., Roy, D. P., Humber, M. L., and Justice, C. O.: The Collection 6 MODIS burned area mapping algorithm and product, *Remote Sens. Environ.*, 217, 72–85, <https://doi.org/10.1016/j.rse.2018.08.005>, 2018.
- Hély, C., Caylor, K., Alleaume, S., Swap, R. J., and Shugart, H. H.: Release of gaseous and particulate carbonaceous compounds from biomass burning during the SAFARI 2000 dry season field campaign, *J. Geophys. Res.*, 108(D13), 8470,
- 380 <https://doi.org/10.1029/2002JD002482>, 2003.
- Huang, X., Li, M., Li, J., and Song, Y.: A high-resolution emission inventory of crop burning in fields in China based on MODIS Thermal Anomalies/Fire products, *Atmos. Environ.*, 50, 9–15, <https://doi.org/10.1016/j.atmosenv.2012.01.017>, 2012.
- Jin, Q., Wang, W., Zheng, W., Innes, J. L., Wang, G., and Guo, F.: Dynamics of pollutant emissions from wildfires in Mainland China, *J. Environ. Manage.*, 318, 115499, <https://doi.org/10.1016/j.jenvman.2022.115499>, 2022.
- 385 Kasischke, E. S., Christensen, N. L., and Stocks, B. J.: Fire, Global Warming, and the Carbon Balance of Boreal Forests, *Ecol. Appl.*, 5, 437–451, <https://doi.org/10.2307/1942034>, 1995.



- Kelly, R., Chipman, M. L., Higuera, P. E., Stefanova, I., Brubaker, L. B., and Hu, F. S.: Recent burning of boreal forests exceeds fire regime limits of the past 10,000 years, *Proc. Natl. Acad. Sci. U.S.A.*, 110, 13055–13060, <https://doi.org/10.1073/pnas.1305069110>, 2013.
- 390 Langenfelds, R. L., Francey, R. J., Pak, B. C., Steele, L. P., Lloyd, J., Trudinger, C. M., and Allison, C. E.: Interannual growth rate variations of atmospheric CO₂ and its δ¹³C, H₂, CH₄, and CO between 1992 and 1999 linked to biomass burning, *Global Biogeochem. Cy.*, 16, <https://doi.org/10.1029/2001GB001466>, 2002.
- Lasslop, G., Hantson, S., Harrison, S. P., Bachelet, D., Burton, C., Forkel, M., Forrest, M., Li, F., Melton, J. R., Yue, C., Archibald, S., Scheiter, S., Arneth, A., Hickler, T., and Sitch, S.: Global ecosystems and fire: Multi-model assessment of
395 fire-induced tree-cover and carbon storage reduction, *Global Change Biol.*, 26, 5027–5041, <https://doi.org/10.1111/gcb.15160>, 2020.
- Lü, A., Tian, H., Liu, M., Liu, J., and Melillo, J. M.: Spatial and temporal patterns of carbon emissions from forest fires in China from 1950 to 2000, *J. Geophys. Res.*, 111, D05313, <https://doi.org/10.1029/2005JD006198>, 2006.
- Luo, Y., Zhang, Z., Li, Z., Chen, Y., Zhang, L., Cao, J., and Tao, F.: Identifying the spatiotemporal changes of annual
400 harvesting areas for three staple crops in China by integrating multi-data sources, *Environ. Res. Lett.*, 15, 074003, <https://doi.org/10.1088/1748-9326/ab80f0>, 2020.
- McGuire, A. D., Sitch, S., Clein, J. S., Dargaville, R., Esser, G., Foley, J., Heimann, M., Joos, F., Kaplan, J., Kicklighter, D. W., Meier, R. A., Melillo, J. M., Moore, B., Prentice, I. C., Ramankutty, N., Reichenau, T., Schloss, A., Tian, H., Williams, L. J., and Wittenberg, U.: Carbon balance of the terrestrial biosphere in the Twentieth Century: Analyses of CO₂, climate,
405 and land use effects with four process-based ecosystem models, *Global Biogeochem. Cy.*, 15, 183–206, <https://doi.org/10.1029/2000GB001298>, 2001.
- Phillips, C. A., Rogers, B. M., Elder, M., Cooperdock, S., Moubarak, M., Randerson, J. T., and Frumhoff, P. C.: Escalating carbon emissions from North American boreal forest wildfires and the climate mitigation potential of fire management, *Sci. Adv.*, 8, eabl7161, <https://doi.org/10.1126/sciadv.abl7161>, 2022.
- 410 Qiu, X., Duan, L., Chai, F., Wang, S., Yu, Q., and Wang, S.: Deriving High-Resolution Emission Inventory of Open Biomass Burning in China based on Satellite Observations, *Environ. Sci. Technol.*, 50, 11779–11786, <https://doi.org/10.1021/acs.est.6b02705>, 2016.
- Rogelj, J., Popp, A., Calvin, K. V., Luderer, G., Emmerling, J., Gernaat, D., Fujimori, S., Strefler, J., Hasegawa, T., Marangoni, G., Krey, V., Kriegler, E., Riahi, K., Van Vuuren, D. P., Doelman, J., Drouet, L., Edmonds, J., Fricko, O.,
415 Harmsen, M., Havlík, P., Humpenöder, F., Stehfest, E., and Tavoni, M.: Scenarios towards limiting global mean temperature increase below 1.5 °C, *Nature Clim. Change*, 8, 325–332, <https://doi.org/10.1038/s41558-018-0091-3>, 2018.
- Shan, Y., Guan, D., Zheng, H., Ou, J., Li, Y., Meng, J., Mi, Z., Liu, Z., and Zhang, Q.: China CO₂ emission accounts 1997–2015, *Sci. Data*, 5, 170201, <https://doi.org/10.1038/sdata.2017.201>, 2018.
- Ministry of Ecology and Environment of the People's Republic of China. Technical Guidelines for Compiling Emission
420 Inventory of Air Pollutants from Biomass Combustion Sources, 2015.



- National, M.: Daily meteorological dataset of essential meteorological elements of China National Surface Weather Station (V3.0)(1951-2010). National Tibetan Plateau / Third Pole Environment Data Center, 2019.
- Shiraishi, T., Hirata, R., and Hirano, T.: New Inventories of Global Carbon Dioxide Emissions through Biomass Burning in 2001-2020, *Remote Sensing*, 13, 1914, <https://doi.org/10.3390/rs13101914>, 2021.
- 425 Su, Y., Guo, Q., Xue, B., Hu, T., Alvarez, O., Tao, S., and Fang, J.: Spatial distribution of forest aboveground biomass in China: Estimation through combination of spaceborne lidar, optical imagery, and forest inventory data, *Remote Sen. Environ.*, 173, 187–199, <https://doi.org/10.1016/j.rse.2015.12.002>, 2016.
- Tian, X., McRae, D. J., Jin, J., Shu, L., Zhao, F., and Wang, M.: Wildfires and the Canadian Forest Fire Weather Index system for the Daxing'anling region of China, *Int. J. Wildland Fire*, 20, 963, <https://doi.org/10.1071/WF09120>, 2011.
- 430 Van Der Werf, G. R., Randerson, J. T., Collatz, G. J., Giglio, L., Kasibhatla, P. S., Arellano, A. F., Olsen, S. C., and Kasischke, E. S.: Continental-Scale Partitioning of Fire Emissions During the 1997 to 2001 El Niño/La Niña Period, *Science*, 303, 73–76, <https://doi.org/10.1126/science.1090753>, 2004.
- Van Der Werf, G. R., Randerson, J. T., Giglio, L., Collatz, G. J., Mu, M., Kasibhatla, P. S., Morton, D. C., DeFries, R. S., Jin, Y., and Van Leeuwen, T. T.: Global fire emissions and the contribution of deforestation, savanna, forest, agricultural, and
435 peat fires (1997–2009), *Atmos. Chem. Phys.*, 10, 11707–11735, <https://doi.org/10.5194/acp-10-11707-2010>, 2010.
- Van Der Werf, G. R., Randerson, J. T., Giglio, L., Van Leeuwen, T. T., Chen, Y., Rogers, B. M., Mu, M., Van Marle, M. J. E., Morton, D. C., Collatz, G. J., Yokelson, R. J., and Kasibhatla, P. S.: Global fire emissions estimates during 1997–2016, *Earth Syst. Sci. Data*, 9, 697–720, <https://doi.org/10.5194/essd-9-697-2017>, 2017.
- Van Wees, D., Van Der Werf, G. R., Randerson, J. T., Andela, N., Chen, Y., and Morton, D. C.: The role of fire in global
440 forest loss dynamics, *Global Change Biol.*, 27, 2377–2391, <https://doi.org/10.1111/gcb.15591>, 2021.
- Wang, S. X. and Zhang, C. Y.: Spatial and Temporal Distribution of Air Pollutant Emissions from Open Burning of Crop Residues in China, *Sciencepaper Online*, 3, 329–333, 2008 (in Chinese).
- Wang, Z., Wang, Z., Zou, Z., Chen, X., Wu, H., Wang, W., Su, H., Li, F., Xu, W., Liu, Z., and Zhu, J.: Severe Global Environmental Issues Caused by Canada's Record-Breaking Wildfires in 2023, *Adv. Atmos. Sci.*, s00376-023-3241-0,
445 <https://doi.org/10.1007/s00376-023-3241-0>, 2023.
- Wotawa, G. and Trainer, M.: The Influence of Canadian Forest Fires on Pollutant Concentrations in the United States, *Science*, 288, 324–328, <https://doi.org/10.1126/science.288.5464.324>, 2000.
- Wu, C., Liu, X., Lin, Z., Rahimi-Esfarjani, S. R., and Lu, Z.: Impacts of absorbing aerosol deposition on snowpack and hydrologic cycle in the Rocky Mountain region based on variable-resolution CESM (VR-CESM) simulations, *Atmos. Chem. Phys.*, 18, 511–533, <https://doi.org/10.5194/acp-18-511-2018>, 2018.
- 450 Xie, X., Zhang, Y., Liang, R., Chen, W., Zhang, P., Wang, X., Zhou, Y., Cheng, Y., and Liu, J.: Wintertime Heavy Haze Episodes in Northeast China Driven by Agricultural Fire Emissions, *Environ. Sci. Technol. Lett.*, 11 (2), 150–157, <https://doi.org/10.1021/acs.estlett.3c00940>, 2024.



- Xu X, Liu J., Zhang S., Li R., Yan C., Wu S.: China's multi-period land use land cover remote sensing monitoring dataset (CNLUCC). Data Registration and Publishing System of the Resource and Environmental Science Data Center of the Chinese Academy of Sciences, (<http://www.resdc.cn/DOI>) DOI: 10.12078/2018070201, 2018.
- 455 Yin, L., Du, P., Zhang, M., Liu, M., Xu, T., and Song, Y.: Estimation of emissions from biomass burning in China (2003–2017) based on MODIS fire radiative energy data, *Biogeosciences*, 16, 1629–1640, <https://doi.org/10.5194/bg-16-1629-2019>, 2019.
- 460 Yin S., He G., Zhang X.: Forest aboveground biomass products in China, 2013-2021[DS/OL]. V1. Science Data Bank, 2023[2024-02-20]. <https://cstr.cn/31253.11.sciencedb.07122>. CSTR:31253.11.sciencedb.07122.
- Zhang, W., Shao, H., Sun, H., Zhang, W., and Yan, Q.: Optimizing Carbon Sequestration in Forest Management Plans Using Advanced Algorithms: A Case Study of Greater Khingan Mountains, *Forests*, 14, 1785, <https://doi.org/10.3390/f14091785>, 2023.
- 465 Zhang, Y., Shao, M., Lin, Y., Luan, S., Mao, N., Chen, W., and Wang, M.: Emission inventory of carbonaceous pollutants from biomass burning in the Pearl River Delta Region, China, *Atmos. Environ.*, 76, 189–199, <https://doi.org/10.1016/j.atmosenv.2012.05.055>, 2013.
- Zhou, Y., Xing, X., Lang, J., Chen, D., Cheng, S., Wei, L., Wei, X., and Liu, C.: A comprehensive biomass burning emission inventory with high spatial and temporal resolution in China, *Atmos. Chem. Phys.*, 17, 2839–2864, 470 <https://doi.org/10.5194/acp-17-2839-2017>, 2017.